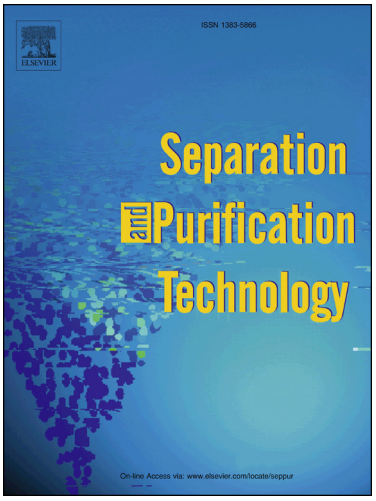

Hydrocyclone equivalent settling area factor at higher concentrations and developing a performance chart

Reza Sabbagh, Charles R. Koch, Michael G. Lipsett, David S. Nobes

PII: S1383-5866(16)31797-X
DOI: http://dx.doi.org/10.1016/j.seppur.2017.02.054
Reference: SEPPUR 13639

To appear in: *Separation and Purification Technology*

Received Date: 22 September 2016
Accepted Date: 24 February 2017

Please cite this article as: R. Sabbagh, C.R. Koch, M.G. Lipsett, D.S. Nobes, Hydrocyclone equivalent settling area factor at higher concentrations and developing a performance chart, *Separation and Purification Technology* (2017), doi: http://dx.doi.org/10.1016/j.seppur.2017.02.054

Hydrocyclone equivalent settling area factor at higher concentrations and developing a performance chart

Reza Sabbagh, Charles R. Koch, Michael G. Lipsett, David S. Nobes*

The Department of Mechanical Engineering, University of Alberta, Edmonton, Alberta T6G 1H9, Canada

Abstract

The equivalent settling area factor allows for comparison amongst different centrifuge separators. For hydrocyclones, the so far developed factor does not consider the effect of concentration of solid particles c in the feed stream, because particle interactions at high concentrations cause hindered settling and reduce hydrocyclone performance. The focus of this paper is a modification of this factor to allow prediction of the influence of higher particle concentration in the feed stream. In particular, the equivalent area factor is modified at high particle concentration by applying different forms of hindered settling concentration functions and using data obtained from experiment or from existing empirical correlations. This results in a set of modified models that are evaluated using statistical techniques. Through statistical analysis, the function $f(c) = c^{0.0488}\exp(-9.445c)$ is selected to modify the equivalent settling area for hydrocyclones. A performance chart is developed for hydrocyclones by undertaking the modified equivalent area model that can be used in hydrocyclone design applications. The developed performance chart is validated and is shown to be capable of predicting the hydrocyclone performance over a wide range of hydrocyclone flow rates and separation cut sizes. This chart is compared with a performance chart available in the literature and the chart in the literature is shown to over-predict the hydrocyclone performance.

*Corresponding author: David. S. Nobes, Mechanical Engineering Department, University of Alberta, Edmonton AB, CANADA
E-mail: david.nobes@ualberta.ca

Keywords: hydrocyclone; performance; concentration; equivalent settling area; design; modeling
2015 MSC: 00-01, 99-00

1. Introduction

The equivalent settling area factor has been developed as a mathematical tool to compare the performance of different centrifugal separators [1–3]. This factor allows comparison and scale-up of centrifugal separators, which is important in the selection and design process. The equivalent settling area factor is defined in relation with flow rate Q and particle settling velocity v_g such that [1]:

$$Q = 2v_g\Sigma \tag{1}$$

and

$$v_g = \frac{\Delta\rho d^2 g}{18\mu} \tag{2}$$

where $\Delta\rho$ is the density difference between liquid and solid, d is the particle diameter (which is typically 50% cut size particle size), and μ is the fluid viscosity.

The factor is also developed for solid-liquid separation in hydrocyclones [4–8] and can be used as a criterion for comparing the hydrocyclone performance with other types of centrifugal separators. This factor in hydrocyclones is based on residence time theory [9], which in turn predicts the 50% cut size particle in separation. The importance of developing such a factor for hydrocyclones and its application in centrifugal technology is detailed in [7, 8]. The version of the equivalent settling area model (ESAM) developed to date [8] does not consider the effect of concentration of solid particles in the feed stream.

It has been observed that the performance of a hydrocyclone is affected by the solids concentration in the feed. A high concentration of solids in the hydrocyclone leads to lower settling velocity [10] as compared to the Stokes settling velocity. The influence of inlet solid concentration on the hydrocyclone performance has been studied theoretically and experimentally [11, 12]. Increasing

the feed concentration while keeping all other parameters constant results in more particles in the overflow and coarser particles in the underflow [11]. This has been attributed to hindered particle motion in the radial direction where particles move toward the wall [11]. Limited capacity of the underflow diameter and changes in the flow field [13] are listed as other reasons for entrainment of the particles in the hydrocyclone. This eventually leads to less efficient separation. A reduction in pressure drop at higher flow rates has also been related to the effect of hindered settling [11].

To correlate the influence of the hydrocyclone design and operating variables, including solids concentration in the feed, several studies have been undertaken. Lynch et al. [14] and Plitt [15] developed empirical models that are widely used in hydrocyclone development. Such models are generally restricted to the specific hydrocyclone dimensions, range of operation, and material properties used to parameterize the model. For instance, the Plitt model has been reported to be incapable of predicting the pressure drop and corrected cut size with low solid fraction in some experiments [16, 17]. While some correlations represent the concentration effect through a function obtained from the regression analysis (as in Plitt model), in some researches the settling velocity of the particles is modified for the hindered conditions. Using the ratio of free to hindered terminal settling velocity for spherical particles [18], a set of correlations with constant coefficients only depend on feed solid characteristics was developed [19].

For families of geometrically similar hydrocyclones, including Bradley and Rietema hydrocyclones, a model is generated based on dimensionless groups to predict hydrocyclones performance [20]. Although this model is limited to certain aspect ratios and hydrocyclone diameters from 22 to 122 mm, it has the advantage that it does not need to be adjusted for each application. Therefore, similar to the Plitt model [15], it is a useful model that can be applied irrespective of the material fed into the hydrocyclone. However, the Coelho model [20] is expected to give a better prediction for the materials used in model development. Feed volumetric solid fraction varies from 0 to 0.1 for this model which - unlike some other models - allows prediction of the performance for low concen-

trations. This model has been reported [20] to be capable of reproducing data from Kelsall [21], Bradley [22] and Rietema [23–26].

An extensive investigation for the effect of solid concentration and other influential factors has been undertaken by researchers at the Julius Kruttschnitt Mineral Research Centre (JKMRC) at the University of Queensland [27–30]. Using the data of JKMRC with the feed solid weight fraction of 14-70% and hydrocyclone diameter ranging from 10-75 cm, a model that includes the effect of hydrocyclone inclination is described [31]. Combining a variety of experimental data sources for small- and large-scale hydrocyclones and undertaking a computational fluid dynamic (CFD) simulation, a semi-mechanistic model has been developed for hydrocyclones based on multiple linear fitting approach for estimating model parameters [32]. A set of application-dependent system constants has also been inserted into the model that must be determined for each new application. This model takes the effect of feed volume concentration into account, including the equation proposed for hindered velocity [18].

The performance of centrifugal separators is typically compared through the equivalent settling area factor [7, 33]. This is the area of a gravity settling tank that yields the same performamce as the centrifugal separator device under the same operating conditions. The performance of hydrocyclones as a type of centrifugal separator in terms of the equivalent settling area at high particle concentration has not been studied. Considering the Stokes flow and a cut size particle in a hydrocylone, an equivalent settling area model has been developed [8]. This model can be extended for the influence of solid concentration in the feed stream.

Typically, increasing the concentration brings the particles closer to each other, which in turn allows them to cluster. This should increase the settling velocity; however, for flows such as in hydrocyclones where the shear rate is high, the cluster does not survive and the settling rate reduces with increasing concentration [34]. Increasing the inlet solid fraction results in a decrease in the separation efficiency [35]. High solid concentration increases the particle-particle interactions and hence reduces the particle settling velocity to what is

known as the hindered settling velocity [11]. This velocity is usually related to the Stokes settling velocity [10] and is a function of concentration [36] such that:

$$v_h = v_g f(c) \tag{3}$$

where v_h represents the hindered settling velocity, f is a function of concentration and c is the fraction of solid volume concentration in the mixture [37]. A well-known relation for the effect of concentration on Stokes (gravitational) settling velocity has been proposed by Richardson and Zaki [38]. It has been observed that the settling velocity changes with changes in the solid fraction c in the mixture such that the Stokes settling velocity v_g is corrected by the multiplicative factor $(1-c)^k$, where k is a coefficient that is experimentally determined to be 4.65 [38]. Other research works have also addressed this subject [18, 36, 39–41]. A method for determining k is presented in [40] which is dependent on the solid material properties and may vary significantly from what is suggested by Richardson and Zaki [38]. For sand particles, a review of the settling models can be found in Zeidan et al. [37].

Modeling the effect of solid concentration in hydrocyclones has been done in the literature by applying a function of solid volume fraction in the mixture c into a hydrocyclone performance model [20, 42–45]. Some investigators have adopted the Richardson and Zaki [38] hindered settling correlation into their hydrocyclone models [42, 46] while others have formed different nonlinear relationships from a gravity settling formulation [44, 47]. Most models are based on experimental correlations as the theoretical solution for the effect of hindered settling is complex. The experiments and resulting experimental correlations for sets of different designs of hydrocyclones, [20] shows that concentration affects the hydrocyclone performance parameters (such as pressure drop, flow rate, and cut size).

The developed ESAM [6–8] is based on residence time theory, which does not take the concentration and hence hindering effect into account, such that:

$$\Sigma = \beta \frac{L \Delta P}{\rho g} \tag{4}$$

and

$$\beta = \frac{\pi n [1 - (D_o/D)^2]}{(D/D_o)^{2n} - 1} \left(\frac{1}{1 - D_i/D} \right)^{2n+1} \tag{5}$$

where Σ is the equivalent area factor from ESAM, ΔP is pressure drop, ρ is liquid density, L is hydrocyclone total length, D_o is overflow pipe diameter, D_i is inlet pipe diameter, D is the diameter of the cylindrical portion of the hydrocyclone, and n is an experimental exponent that appears in the tangential velocity component [9]. The equivalent diameter to a circular pipe is used in Eq. (5) by equating the inlet section area to the area of a circular pipe. Mathematically Eq. (5) is valid if the following conditions hold: $D_o/D > 0$, $D_i/D < 1$, and $D_o/D \neq 1$. Physically, $(2D_i/D + D_o/D) \leq 1$ can be considered to be a limit for the inlet pipe and the vortex finder diameters [6, 8].

This study modifies the ESAM, Eq. (4), to allow predicting the separation performance at high concentrations when hindered settling occurs. This is done by applying different forms of hindered settling concentration functions in the ESAM. The function that provides the best prediction is obtained through regression analysis by comparisons between the empirical data and predictive models. The modified equivalent settling area model (modified ESAM) for the effect of concentration is denoted as Σ_c and is used to evaluate the effect of operating and performance parameters in hydrocyclones. This model (Σ_c) is used to develop a performance guideline chart for hydrocyclones. The hydrocyclone separation cut size and centrifugal acceleration is also evaluated using Σ_c.

2. Methodology

2.1. Hindered settling functions

Hindered settling is typically described by introducing a function of the solid volume concentration $f(c)$ as outlined in Eq. (3). Different functional forms of $f(c)$ that have been used in hydrocyclone studies in the literature are listed in

Table 1: Concentration models $f(c)$ for the effect of solid concentration on the hydrocyclone performance.

Case	Function	Reference
$f_1(c)$	$(1-c)^{\alpha}$	[38]
$f_2(c)$	$c/(1-c)^{\alpha}$	[48]
$f_3(c)$	$10^{\alpha c}/(1-c)^{\beta}$	[18]
$f_4(c)$	$\exp(\alpha c)$	[49]
$f_5(c)$	$(1-c)(1-c/\beta)^{\alpha}$	[50]
$f_6(c)$	$c^{\alpha}/(1-c)^{\beta}$	[43]
$f_7(c)$	$c^{\beta}\exp(\alpha c)$	current study

Table 1. The functions either modify the radial terminal velocity of the particles in the hydrocyclone or predict the separation cut size in the device, which in turn is related to the settling velocity. The last function in the table is proposed by the current study and is included in this table for completeness.

Each of these functions is evaluated to examine how it modifies the ESAM with concentration. Each function is then combined with the ESAM and the resulting relation (a modified model) is used to predict the equivalent settling area factor in a hydrocyclone for different concentrations. The predicted data is then compared with data derived from empirical correlations for separation ranges from low (1%v/v) to high solids concentration (up to 45%v/v) and the capability of the modified model (and the concentration function) in predicting the equivalent area factor under the influence of solids concentration is examined. The theoretical equivalent settling area model ESAM is modified as $\Sigma_c = \Sigma f(c)$ using a concentration function $f(c)$. Least-squares regression is used to determine the function coefficient(s) (α or β) listed in Table 1. The results are then compared and the function with the best fit is selected.

2.2. Model parametrization

Experimental data [6, 8] and data obtained from emprical correlations are used to parametrize and evaluate the model. For the experiments, a 5 cm Krebs geometry hydrocyclone [6, 8] is run with soda-lime glass-bead particles. Flow from a mixing tank is pumped to the hydrocyclone using a centrifugal pump. A progressive cavity pump is connected to the underflow pipe and returns the underflow to the mixing tank. The inlet particle cut sizes and the separation particle cut size are obtained by particle size analyzing for the samples taken from the inlet and underflow of the hydrocyclone, respectively. The inlet flow rate in the test is measured using a Coriolis flow meter. To obtain the pressure drop, the pressure sensors are used to record the pressure at each inlet or outlet pipe. Such information is reuired for obtaining the experimental equivalent area factor. Further details of the experimental setup can be found in [6, 8] with the test conditions listed in Table 2. As can be seen from Table 2, solids concentration is less than 2 %v/v.

Since the experiments are limited to low solid concentrations, the required data at higher concentrations to develop and evaluate the concentration functions are obtained from empirical correlations available in the literature. Correlations developed in [32] (C1) and [20] (C2) are used in the present work, as each of these covers a certain range of solid fraction in the feed stream and each correlation has some limitations, as discussed in section 1. Therefore, before using C1 and C2, these two models are evaluated using data reported in [51, 52] for different hydrocyclones and materials. The details, including the hydrocyclone dimensions and operating conditions, are listed in Table A.1 and Table A.2 in the appendix.

For a hydrocyclone with known dimensions, both flow rate and separation cut size are calculated from the correlations (C1 or C2) or obtained from our experimental data. Using the cut size, flow properties, and operating variables, the settling velocity of the particles is obtained from Eq. (2). Equivalent settling area factor is then obtained from Eq. (1) since it is proportional to settling velocity through flow rate [1, 2]. The flow rate is determined either from the ex-

Table 2: Experimental conditions

Parameter	Condition
Centrifugal pump speed (Hz)	40, 50, 60
Underflow progressive cavity pump speed (Hz)	10 to 50
Inlet pressure (kPa)	150 to 230
Inlet flow rate (m^3/hr)	1 to 2.4
Inlet solid volume concentration (v/v)	0.001 to 0.02
Solid density (kg/m^3)	2500
Liquid density (kg/m^3)	998

Table 3: Values of the variables for calculating data from correlations C1 and C2.

Variable	Value	Units
Liquid density, ρ	997	kg/m^3
Liquid viscosity, μ	0.00097	Pa.s
Solid density, ρ_s	2770	kg/m^3
Pressure drop, ΔP	30-140	kPa
Inlet concentration, c	0.0125-0.45	m^3/m^3

perimental data or is obtained from the empirical correlations. The calculation method is described in detail in [7]. The calculation procedure is repeated for different inlet concentrations and pressure drops. The experimental data and results from correlations C1 or C2 are simply called data; and the calculated settling area factor from the experimental data (or correlations) is referred to as a calculated factor from data, and denoted Σ_{data}.

3. Results and Discussion

3.1. Evaluation of C1 and C2

The predicted flow rate and cut size from correlations C1 and C2 are examined against experimental data obtained from [51, 52] and are shown in Fig. 1 and Fig. 2 for 19 cases listed in Table A.1 and Table A.2 in the appendix. The

C1 correlations have material dependent terms to correct the predicted flow rate and cut size for the material properties that do not appear in the correlations, such as particle shape. The results for C1 shown in Fig. 1 and Fig. 2 are given first for the case when there is no correction for material dependent terms (shown as no correction in the figures) and then shown with correcting values for each material (shown as corrected in the figures). After identifying the values of the material dependent parameters, C1 can be used to modify ESAM for the effect of concentration for all of the test conditions in Table 2. It can be seen from Fig. 1 and Fig. 2 that the corrected C1 predicts the flow rate and cut size better than C2 for all cases listed in Table A.1. For C2 the flow rate and the cut size for cases 10 to 17 (where test dust is used in water, see Table A.1) is predicted closely; but there are noticeable discrepancies for other cases. Based on this evaluation for C1 and C2, the test conditions of cases 10 to 17 (well predicted using both models C1 and C2) are used to develop a modified ESAM. These conditions are applied to correlations from C1 and C2 for the hydrocyclone design and sizes within the limits of the models. The effect of concentration on ESAM is investigated for low concentrations (1-10 %v/v) using C2 and for both low and high concentrations (1-45 %v/v) are investigated using C1. The data points used in modifying ESAM are generated for different hydrocyclones types and diameter. Such conditions are detailed in Table A.3. Combination of the conditions listed in Table A.3 provides 5040 data points for every hydrocyclone type.

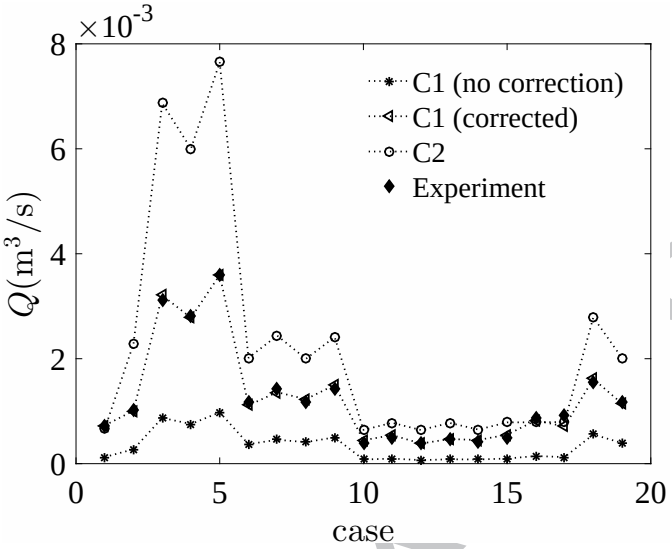

Figure 1: Accuracy of the correlations C1 and C2 in predicting the experimental flow rate; experimental data is from [51, 52].

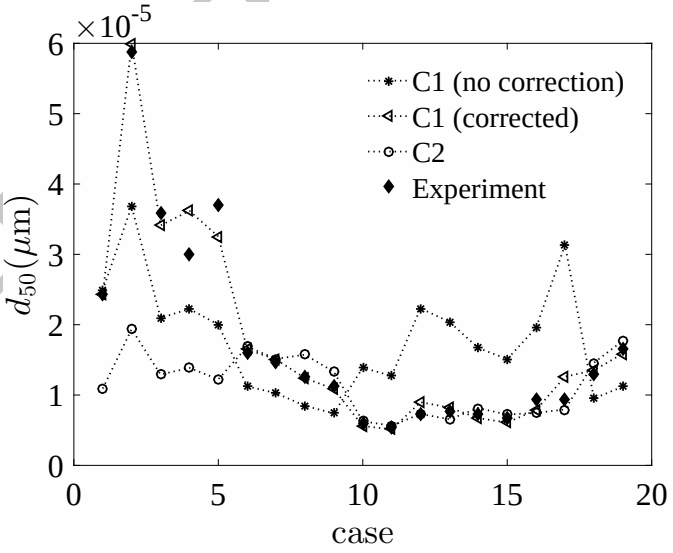

Figure 2: Accuracy of the correlations C1 and C2 in predicting the experimental cut size; experimental data is from [51, 52].

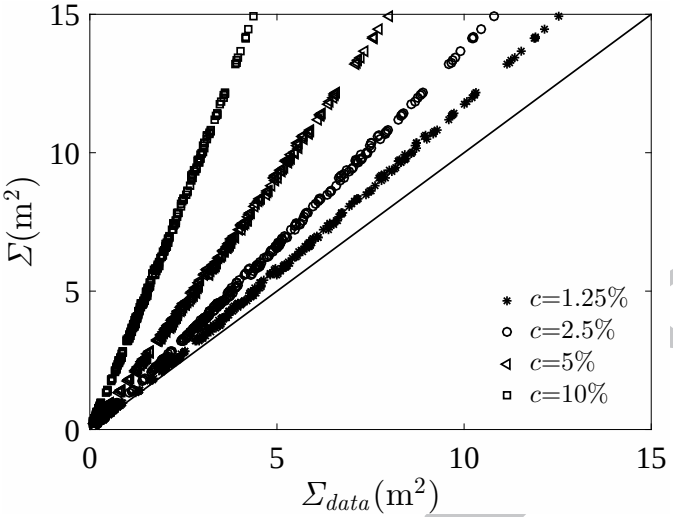

Figure 3: Comparison of the predicted (Eq. (4) and Eq. (5)) and calculated equivalent area factor from C2 at different solid volume concentration (Σ_{data}) for a Bradley hydrocyclone; solid line is for $c < 0.01$.

3.2. Effect of concentration on ESAM

The effect of increasing the inlet concentration on the equivalent area is presented for the case of a Bradley hydrocyclone. The calculated data from C2 for different solid volume concentrations varying from 1.25% to 10% is compared to the predicted values from the ESAM (Eq. (4) and Eq. (5)) as shown in Fig. 3. Increasing the amount of solids in the inlet flow decreases the equivalent area factor, which is the effect that is not included in the ESAM. Increasing the concentration causes the ESAM to overpredict the equivalent area factor Σ. The same trend is also found for higher solid concentrations for Rietema and Demco 4H hydrocyclones [6].

3.3. Modifying ESAM

Nonlinear regression for equation $\Sigma_c = \Sigma f(c)$ and the functions listed in Table 1 are used to modify the ESAM to fit to the same data. Table 4 gives regression results for all data obtained for different hydrocyclone types and for hydrocyclone diameters ranging from 1 to 100 cm. To test whether the

Table 4: Regression results for ranges of hydrocyclone designs and diameters.

Variable	$f_1(c)$	$f_2(c)$	$f_3(c)$	$f_4(c)$	$f_5(c)$	$f_6(c)$	$f_7(c)$
α	12.222	-2.0906	-4.640	-12.751	6.525	-0.051	-9.445
β	-	-	2 (fixed)	-	0.6 (fixed)	-8.818	0.0488
SE	0.039	0.151	0.017	0.037	0.024	α: 0.000 β: 0.011	α: 0.011 β: 0.000
t-statistics	315.8 8	-19.23	-281.06	-1467	-340.26	α: 380.17 β: -784.66	α: -849.84 β: 381.42
p-value	0	1.83E-81	0	0	0	α: 0; β: 0	α: 0; β: 0
R^2	0.958	-0.160	0.962	0.962	0.955	0.996	0.997
RMS error	9.03	47.37	8.61	8.53	9.37	2.68	2.52
RSS	1.23E6	3.39E7	1.12E6	1.10E6	1.33E6	1.08E5	9.62E4
AIC	54719	79786	54014	53871	55277	36335	35442

coefficient (α or β) of the function is statistically significant in the model, the t-statistic test is used [53]. The probability of there being no difference between the groups using the concentration function $f(c)$ and observed data is measured by the p-value [53]. Also presented in Table 4, measures to evaluate the goodness of the fit to the data through the estimated coefficient(s) and the regression model are: the standard error of the estimates (SE) (which is a measure of the accuracy of predictions), root mean squared (RMS) error (which measures the difference between predicted values by the model and the data), and the coefficient of determination R^2 (which is a measure of how close the values predicted by the model are to the data).

The regression statistics show that most of the models provide a good estimation of the concentration function. The only function that does not closely predict the data well is $f_2(c)$. The determination coefficient R^2 is greater than 0.95 in all models except for $f_2(c)$. Thus, the function $f_2(c)$ is removed from the study. All other models (functions) are statistically significant and the RMS errors are small. The functions $f_6(c)$ and $f_7(c)$ are comparable with a higher

value of R^2 and potentially can be the selected function to modify ESAM. Using the Akaike information criterion [54], it is possible to determine which model is more likely to be true model in regenerating the data. The Akaike information criterion (AIC) is defined as [54]:

$$AIC = N \ln(\frac{RSS}{N}) + 2K \tag{6}$$

where N (=15120) is the number of observations, K (=3) is the number of model parameters (predictors and response) involved in the regression, and RSS is residual sum of squares (sum of the square of the vertical distances of the data points from the fitted curve) and its values are indicated in Table 4. The probability that one candidate model is better than another candidate model is obtained from the AIC values of every two candidate models. The Akaike information criterion AIC is an indication of how much more or less likely a model is to be true [55]. A model with a lower AIC value is the model more likely to be correct and thus such a model has a higher probability of being the true model in comparison to another. Details about the calculations of these statistical parameters can be found in [56].

The AICs of the models in this study are tabulated in Table 4 for the models listed in Table 1. According to Table 4, the AIC score in the model that includes $f_7(c)$ is the lowest amongst all the other candidate models. Considering the function with the lowest AIC (most likely function) in Table 4, the order of the functions (from the most likely function to the least likely function) is as follows: $f_7(c) > f_6(c) > f_4(c) > f_3(c) > f_1(c) > f_5(c)$. Therefore, $f_7(c)$ is expected to be more likely to be the true function in the model and is selected as a basis to develop a modified model for predicting the equivalent area factor. The form of function $f_7(c)$ is obtained after testing several different combinations of all of the other functions and choosing the best predictive function based on AIC. The values for coefficient $\alpha = -9.445$ and $\beta = 0.0488$ from Table 4 for $f_7(c)$ are substituted into $f_7(c)$; and the selected function to be used from the study is:

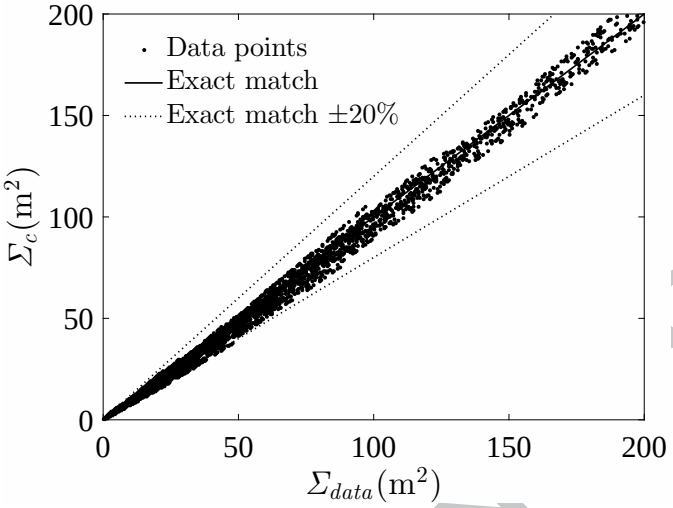

Figure 4: Accuracy of the proposed model (Eq. (8)) in predicting the equivalent area factor; Σ_c from Eq. (8).

$$f(c) = c^{0.0488}\exp(-9.445c) \tag{7}$$

The modified equivalent area factor Σ_c (also called modified model or modified ESAM), including the influence of concentration, is now obtained by combining Eq. (4), Eq. (5), Eq. (7) and $\Sigma_c = \Sigma f(c)$, and by including an application dependent correction factor such that:

$$\Sigma_c = k_s \frac{\pi n[1-(D_o/D)^2]}{(D/D_o)^{2n}-1}\left(\frac{1}{1-D_i/D}\right)^{2n+1}\frac{L\Delta P}{\rho g}c^{0.0488}\exp(-9.445c) \tag{8}$$

where k_s is a coefficient that depends on the material properties and the application.

Since the equivalent settling factor is related to the flow rate and settling velocity of particles (and hence the separation cut size), k_s is expected to be proportional to the flow rate and cut size correction coefficients [32]. The correction coefficient k_s, however, can be parameterized by one or more experimental results. The accuracy of this model for predicting the data used to generate the modified equivalent area factor is evaluated for a range of volume concentrations

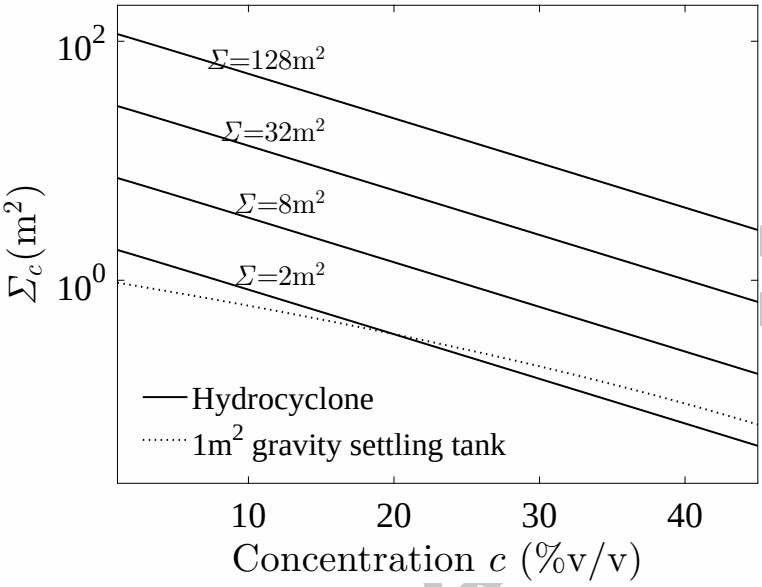

Figure 5: Effect of concentration on modified equivalent area factor Σ_c from Eq. (8); dotted line represents $\Sigma_c = (1-c)^{4.65}$.

from 1.2% to 45% and for different hydrocyclone types and is shown in Fig. 4. The modified equivalent settling area in Eq. (8) is valid for the range of hydrocyclone designs used to develop the model (Bradley, Rietema and Demco 4H) and parameters and conditions listed in Table 3, Table A.1 and Table A.2 as discussed in section 2 and section 3.1.

3.4. Application of Σ_c

The effect of the inlet concentration on Σ_c, using Eq. (8) is shown in Fig. 5. This shows increasing the solid concentration decreases Σ_c and hence the performance of the hydrocyclone. It also shows that for certain solid amounts in the feed flow, the equivalent area factor of the hydrocyclones drops to less than $(1-c)^{4.65}$ m^2 which is the area of a continuous gravity settling tank performs at concentration c where its settling velocity is calculated from Richardson-Zaki correlation [38]. This shows that the hydrocyclone performance may reduce to the performance of a gravity settling tank that has unit area or less (depend-

ing on solids concentration). This can happen to hydrocyclones that have low equivalent area factor at a high solid concentration and may not be desired for a hydrocyclone in operation, considering the cost of manufacturing, installation, and operation compared to a gravity settling tank. To avoid such conditions when a single hydrocyclone is in use, there is a maximum solids concentration that should be used. This maximum value can be determined from Eq. (8) by equating the relation to $(1-c)^{4.65}$ and solving it for c. This concentration is approximately calculated and graphically depicted in Fig. 6, for different Σ values (from Eq. (4)) ranging from 1 to 4 m^2. For example, point A on the figure is a hydrocyclone that has equivalent settling area equal to 3 m^2, which should be operated with less than 26.3%v/v feed solid concentration to perform more efficiently than a gravity settling tank with unit area under the same concentration condition.

Contours of Σ_c are plotted for a 10 cm hydrocyclone of Bradley type and Rietema type in Fig. 7 and Fig. 8 respectively. To achieve the same performance Σ_c in a hydrocyclone when the concentration increases, the pressure drop should be increased. Comparing the two figures, at the same concentration and pressure drop, a Rietema hydrocyclone has a higher equivalent area factor than a Bradley type which is according to what has been reported in [57]. The interaction of the variables in calculating Σ_c for a Bradley and Rietema hydrocyclones are plotted in Fig. 9 and Fig. 10 for a range of hydrocyclone diameters and inlet concentrations and pressure drops from 50 kPa to 300 kPa. As the hydrocyclone diameter increase, Σ_c moves higher. A Bradley hydrocyclone has about 83% of the performance of a Rietema hydrocyclone for the same operating conditions, as shown in Fig. 9 and Fig. 10.

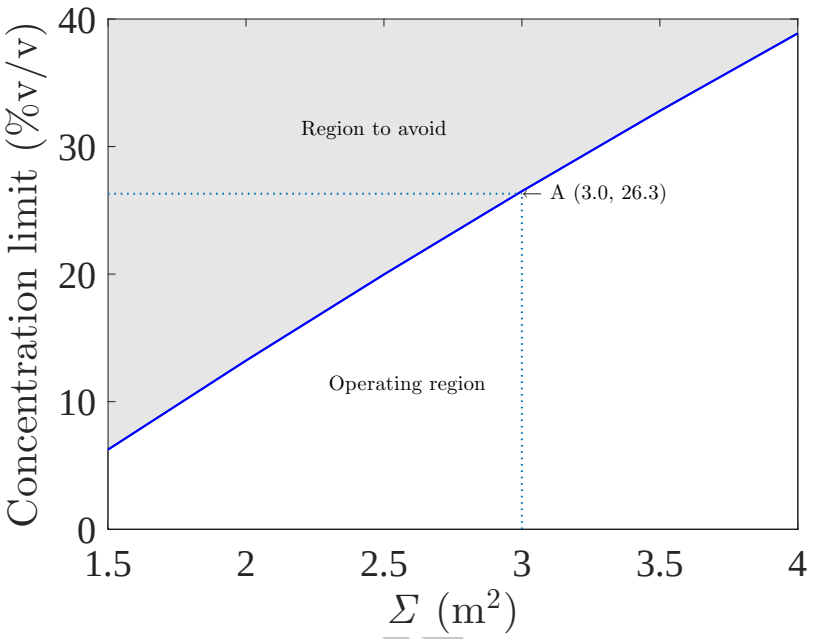

Figure 6: Maximum concentration in hydrocyclone to keep the hydrocyclone performance higher than the performance of a gravity settling tank with unit area under similar concentration conditions; if $c = 0$ then $\Sigma_c = \Sigma$.

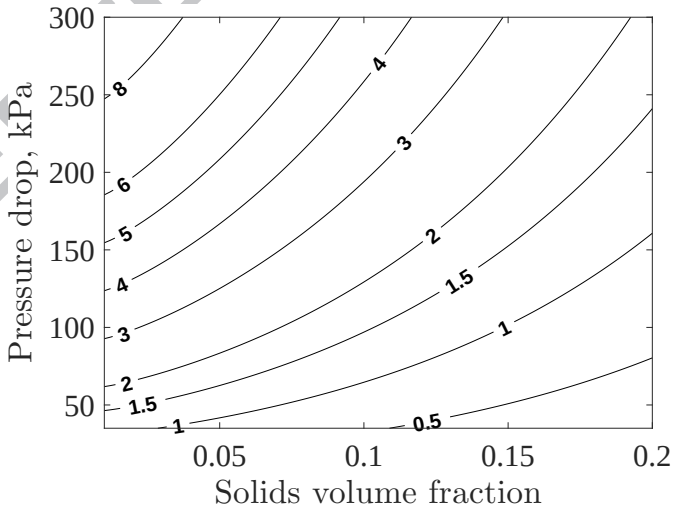

Figure 7: Contours of Σ_c (from Eq. (8)) for a Bradley hydrocyclone with 10 cm diameter.

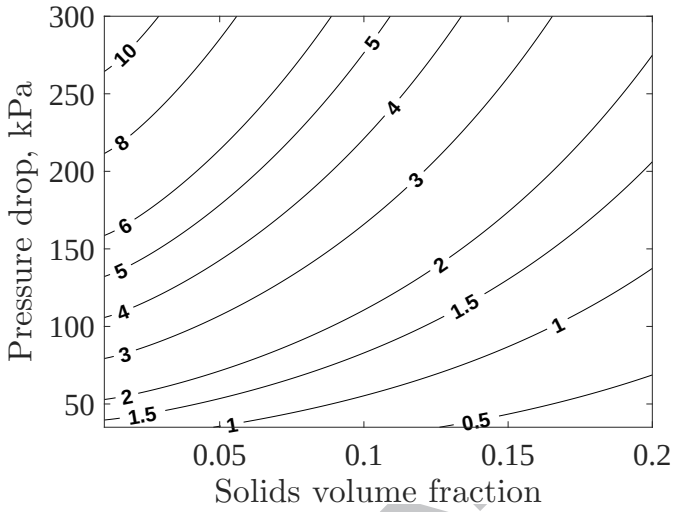

Figure 8: Contours of Σ_c (from Eq. (8)) for a Rietema hydrocyclone with 10 cm diameter.

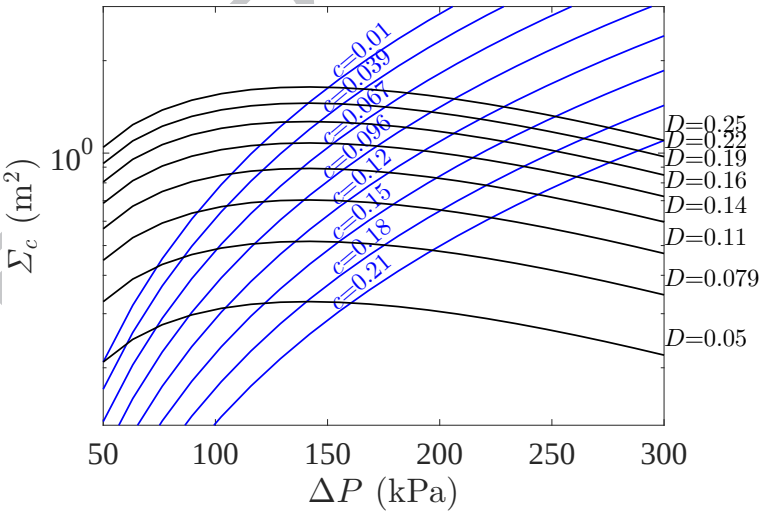

Figure 9: Effect of pressure drop, inlet concentration (fraction) and hydrocyclone diameter on Σ_c in Bradley hydrocyclones; Σ_c from Eq. (8).

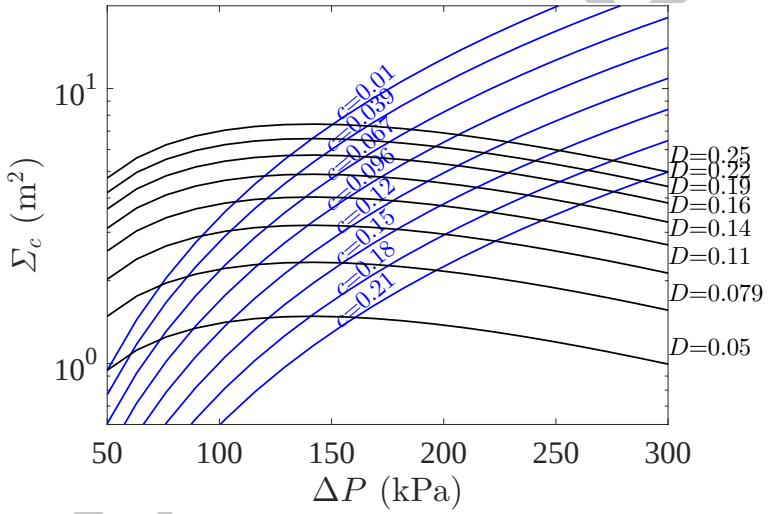

Figure 10: Effect of pressure drop, inlet concentration (fraction) and hydrocyclone diameter on Σ_c in Rietema hydrocyclones; Σ_c from Eq. (8).

3.5. Developing design guidelines for hydrocyclones

The equivalent area factor in hydrocyclones can be used to develop a performance chart to compare hydrocyclones with other separation techniques. Flow rate and particle size (or settling velocity) are parameters of interest in hydrocyclone selection and design. A hydrocyclone performance chart is developed based on these parameters using Eq. (1) and Eq. (2) and replacing Σ in Eq. (1) with Σ_c from the model developed for the equivalent area factor in Eq. (8). For a given hydrocyclone design and fluid density, flow rate Q is calculated for each pressure drop as:

$$Q = \left[\left(\frac{D}{D_o}\right)^{2n} - 1\right]^{-0.5} \left[\frac{n\Delta P}{2^{2n-1}\rho}\right]^{0.5} \frac{D^n H(r_2^{1-n} - r_1^{1-n})}{(1-n)} \tag{9}$$

where H is the height of a rectangualr inlet pipe and r_1 and r_2 are distances between the inlet pipe walls and hydrocyclone centerline. Details of the derivation of Eq. (9)are discussed in [8]. Σ_c is calculated from Eq. (8). Calculating Q and Σ_c, settling velocity v_g is obtained from Eq. (1). Having v_g, the particle cut size diameter can also be determined from Eq. (2). Hydrocyclone diameters for the performance chart development range from 1 to 50 cm and the liquid and solid phase properties in the calculations are listed in Table 3.

3.5.1. Performance charts

Hydrocyclone performance is predicted for pressure drop ranges from 35 kPa to 600 kPa that is the typical range for hydrocyclone applications [9]. The performance lines for Bradley and Rietema type hydrocyclones are shown in Fig. 11 and 12 for three nominal pressure drops and at two different solid volume concentrations $c = 1\%$v/v and $c = 20\%$v/v, respectively. These are shown as flow rate versus twice the settling velocity ($2v_g$). Comparing Fig. 11 and Fig. 12 to each other, it is apparent that, at a constant flow rate and pressure drop, the gravitational settling velocity (x-axis) increases significantly (hence increasing the separation cut size) as the solid concentration increases from 1% to 20%. It should be noted that this settling velocity is an indication of separation cut size

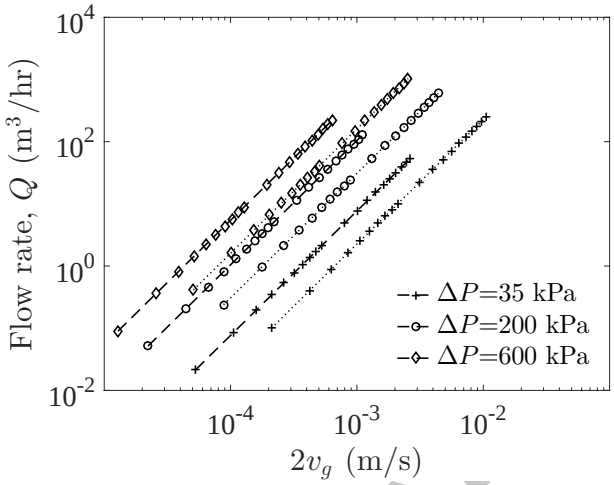

Figure 11: Hydrocyclone performance of a hydrocyclone obtained from equivalent area factor at $c = 1\%$v/v.; dotted line: Rietema hydrocyclone; dashed line: Bradley hydrocyclone

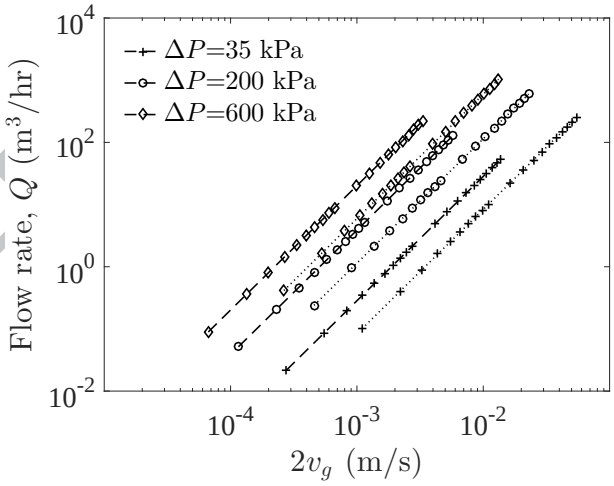

Figure 12: Hydrocyclone performance of a hydrocyclone obtained from equivalent area factor at $c = 20\%$v/v.; dotted line: Rietema hydrocyclone; dashed line: Bradley hydrocyclone

according to Eq. 2 and is not the actual settling velocity of the particles in the hydrocyclone under centrifugal acceleration.

Comparing the performance of Bradley and Rietema hydrocyclones in Fig. 11 and Fig. 12, it is clear that a Rietema hydrocyclone has a higher flow rate and can handle more flow rate than a Bradley hydrocyclone for the same pressure drop, cut size particle and inlet concentration.

Performance curves are generated at different concentrations and pressure drops for different hydrocyclone types (Bradley, Rietema and Demco 4H) to develop a new performance chart. The curves are bounded to obtain a performance chart that covers the wide range of applications for hydrocyclones of different types and sizes and is shown in Fig. 13. Experimental data from our work [6, 8], from the literature [21, 52, 58], data obtained from a hydrocyclone manufacturer (FLSmidth Krebs Hydrocyclone [59]) and data calculated from Plitt's model are used to validate the chart. These experimental and calculated results are all depicted in Fig. 13. Comparing these sets of data with the chart shows that the chart developed from the new model overlaps with the data and hence the chart predicts the hydrocyclone performance well for data within the region of typical experimental data.

The performance of hydrocyclones is also compared with the performance of a continuous gravity settling tank with unit area at low concentration ($c <$ 1 %v/v) and a higher concentration ($c = 20$ %v/v) in Fig. 13. It is important to note that a single hydrocyclone may perform near to or worse than a gravity settling tank for certain operating conditions. Clearly, such conditions should be avoided in hydrocyclone design and operation.

Figure 13 also shows the hydrocyclone performance chart developed by Lavanchy [60]. When the modified performance chart is compared with Lavanchy's performance chart (LPC) [60] the results show that the LPC overpredicts the hydrocyclone performance and cannot be used in hydrocyclones applications. More details about this overprediction can be found in [7]. Therefore, the hydrocyclone performance chart on LPC can be replaced with the modified chart in this research.

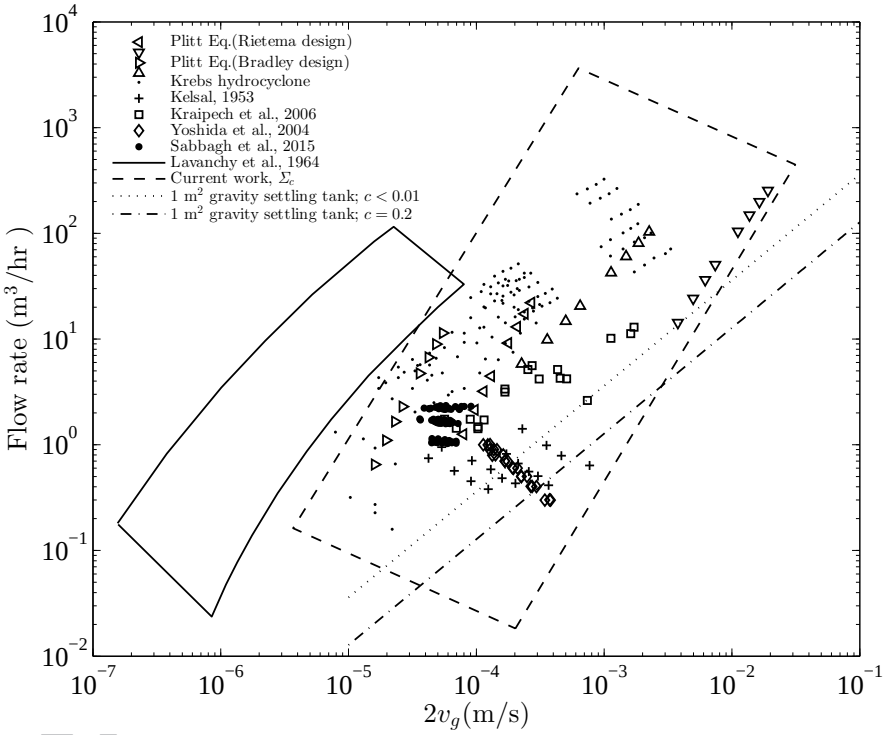

Figure 13: Hydrocyclone modified performance chart compared to data from the literature and to Lavanchy's performance chart [60].

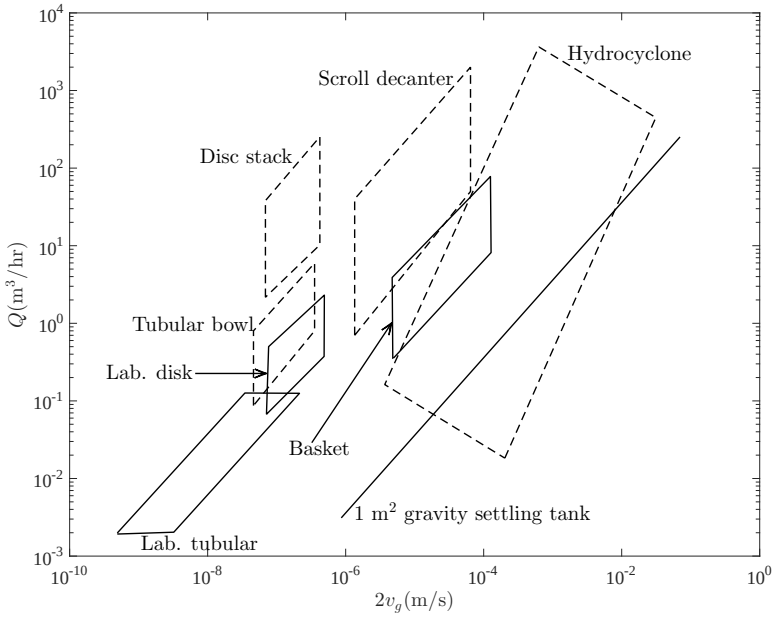

Figure 14: Hydrocyclone modified performance chart compared to centrifuge separator devices.

Comparing the hydrocyclone performance with other centrifugal separators and gravity settling tanks is an important application of the modified performance chart. This is undertaken by combinig the hydrocyclone performance chart developed in the current research with the performance of centrifuge separators from [7, 33] as shown in Fig. 14. Figure 14 presents an update performance chart for centrifugal separators that compares different types of centrifuges with hydrocyclones. This updated performance chart shows that hydrocyclones can be used in a wider range than other centrifuge separators. Having no moving parts, hydrocyclones of different size can be simply made for variety of applications and performance range. However, hydrocyclones applications are limited to a certain settling velocity (affected by particle size, density difference and particle concentration) and cannot perform as well as some other centrifugal techniques.

3.5.2. Separation cut size in hydrocyclones

The effect of the pressure drop and the hydrocyclone diameter on the separation cut size is shown in Fig. 15 and Fig. 16 for Bradley and Rietema hydrocyclones for concentrations $c = 1\%$v/v and $c = 20\%$v/v, respectively. As can be seen, increasing the hydrocyclone diameter or decreasing the pressure drop while the other variable is held constant, results in increasing the cut size. To achieve the same cut size at a constant concentration while the hydrocyclone diameter increases, the pressure drop must be increased. However, creating a high pressure drop may not be always possible due to practical limits or energy/cost concerns, in which case a multiple smaller hydrocyclones is a possible option to process the required throughput.

Comparing the cut size of a Bradley and a Rietema hydrocyclone of the same size in Fig. 15 and Fig. 16 shows that a Bradley hydrocyclone has a smaller cut size than a Rietema hydrocyclone for a similar pressure drop and hydrocyclone diameter. This matches observations in [57] which compares the Bradley and Rietema hydrocyclones based on empirical correlations. Increasing hydrocyclone diameter results in reducing the cut size for both the Bradley and Rietema hydrocyclones. When comparing Fig. 15 and Fig. 16, it is apparent that increasing the inlet concentration results in larger cut size for both the Bradley and the Rietema hydrocyclones. This is due to the effect of hindered settling in hydrocyclones [9] at higher concentrations, which reduces the settling velocity of particles.

The separation cut size is also calculated for the hydrocyclone modified performance chart of Fig. 13, to produce the chart shown in Fig. 17, with the separation cut size values on the second top horizontal axis. The cut size on this axis is obtained from the settling velocity relation Eq. (2) for density difference between solid and liquid equal to 1500 kg/m^3. From Fig. 17, hydrocyclones can be used to separate particles from about 5 μm to about 300 μm, which matches the literature [61].

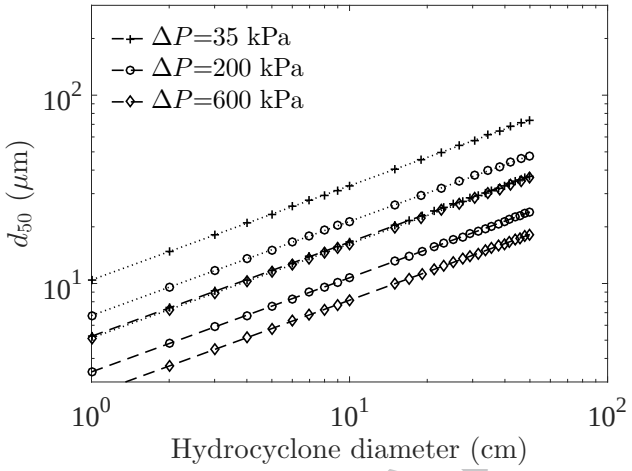

Figure 15: Separation cut size in hydrocyclones; $c = 1\%$v/v.; dotted line: Rietema hydrocyclone; dashed line: Bradley hydrocyclone

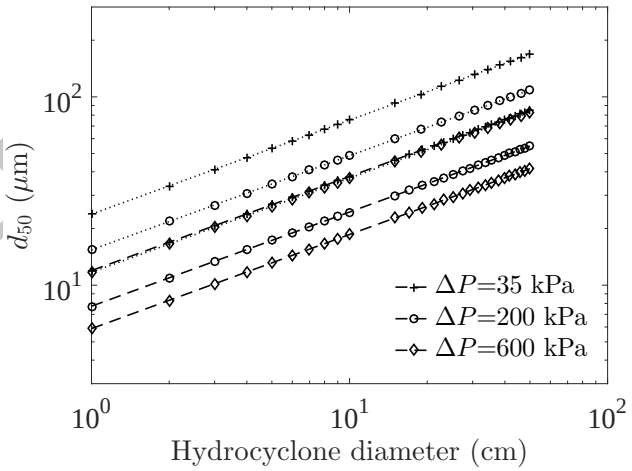

Figure 16: Separation cut size in hydrocyclones; $c = 20\%$v/v.; dotted line: Rietema hydrocyclone; dashed line: Bradley hydrocyclone

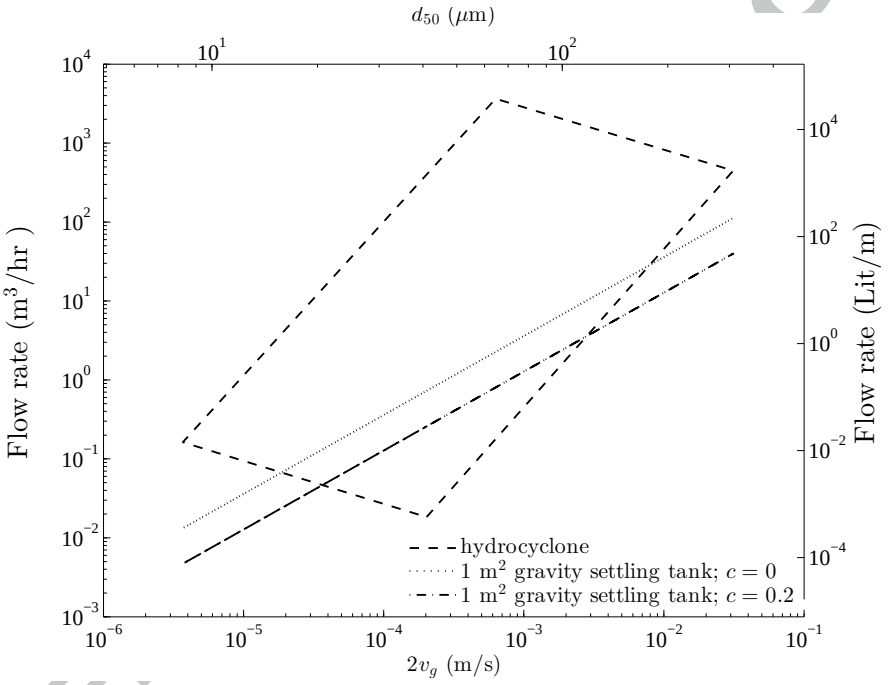

Figure 17: Hydrocyclone modified performance chart compared to gravity settling tank, top horizontal axis: separation cut size for density difference = 1500 kg/m^3.

4. Conclusions

The effect of concentration on separation performance of hydrocyclones has been studied by developing a model for equivalent area factor. The equivalent settling area model (ESAM) is modified by combining it with a function of concentration to include the effect of hindered settling. Different types of particle concentration functions used in the literature for hydrocyclones are evaluated in the current study to predict the equivalent area factor. The predicted factor for each function is compared with a set of data from experimental work or is obtained from empirical correlations. Two different sets of correlations are used to cover a range of low to high concentration and to correct the data for the effect of material properties.

Comparing the data with predictions from the modified models and performing statistical analysis, the function $f(c) = c^{0.0488} \exp(-9.445c)$ is found to match the data and as the best representative function and ESAM is modified. This modification is limited to the hydrocyclone designs investigated in this research and the limits of correlations used in the development. The modified ESAM (Σ_c) is used to develop a modified performance chart for hydrocyclones. The chart is partially validated using experimental data over a limited range of possible operation, and using more extensive data obtained from a hydrocyclone data sheet. The validated modified performance chart can be used to replace previous performance charts in the literature.

5. Acknowledgments

Financial support from the Canada Foundation for Innovation (CFI) and the Natural Sciences and Engineering Research Council of Canada (NSERC) is gratefully acknowledged.

References

[1] C. M. Ambler, The Evaluation of Centrifuge Performance, Chemical Engineering Progress 48 (3) (1952) 150–158.

[2] C. M. Ambler, The theory of scaling up laboratory data for the sedimentation type centrifuge, Journal of biochemical and microbilogical technology and engineering 1 (2) (1959) 185–205. doi:10.1002/jbmte.390010206. URL http://doi.wiley.com/10.1002/jbmte.390010206

[3] C. M. Ambler, The fundamentals of separation, including Sharples Sigma Value for predicting equipment performance, Industrial & Engineering Chemistry 53 (6) (1961) 429–429. doi:10.1021/ie50618a021. URL http://pubs.acs.org/cgi-bin/doilookup/?10.1021/ie50618a021

[4] R. Sabbagh, M. G. Lipsett, C. R. Koch, D. S. Nobes, Theoretical and experimental study of hydrocyclone performance and equivalent settling area, in: Proceedings of the ASME 2014 International Congress & Exposition IMECE2014, Montreal, Canada, ASME, Montreal, Canada, 2014. doi:IMECE2014-37482.

[5] R. Sabbagh, M. G. Lipsett, C. R. Koch, D. S. Nobes, A mathematical model of equivalent settling area for predicting hydrocyclone separation performance, in: European Conference on Fluid Particle Separation-FPS2014, Société Française des Séparations Fluides-Particles, Lyon, France, 2014, pp. 61–62.

[6] R. Sabbagh, Theoretical and experimental investigation of hydrocyclone performance and the influence of underflow pumping effect, Ph.D. thesis, University of Alberta, Edmonton (2015).

[7] R. Sabbagh, M. G. Lipsett, C. R. Koch, D. S. Nobes, Hydrocyclone performance and energy consumption prediction: A comparison with other centrifugal separators, Separation Science and Technology 50 (6) (2015) 788–801. doi:10.1080/01496395.2014.978463.

[8] R. Sabbagh, M. G. Lipsett, C. R. Koch, D. S. Nobes, Predicting equivalent settling area factor in hydrocyclones; a method for determining tangential

velocity profile, Separation and Purification Technology 163 (2016) 341–351. doi:10.1016/j.seppur.2016.03.009.
URL http://linkinghub.elsevier.com/retrieve/pii/S1383586616301137

[9] L. Svarovsky, Hydrocyclones, Holt Rinehart and Winston, 1984.

[10] R. L. Panton, Incompressible Flow, 4th Edition, John Wiley & Sons, Inc. All, 2013.

[11] T. Braun, M. Bohnet, Influence of feed solids concentration on the performance of hydrocyclones, Chem. Eng. Technol. 13 (1990) 15–20.

[12] G. J. C. Childs, W. M. Finch, N. G. Smith, The effect of high concentration on the performance of a hydrocyclone with fine particle feeds, in: Hydrocyclones 96, Wiley, London UK, 1996, pp. 255–262.

[13] J. Severino, Mechanistic modeling of solid-liquid separation in small diameter hydrocyclones, Ph.D. thesis, The University of Tulsa (2007).
URL http://www.tustp.org/publications/Jose_Severino_Thesis_2007.pdf

[14] A. Lynch, T. Rao, C. Bailey, The influence of design and operating variables on the capacities of hydrocyclone classifiers, International Journal of Mineral Processing 2 (1975) 29–37. doi:10.1016/0301-7516(75)90010-1.

[15] L. Plitt, A mathematical model of the hydrocyclone classier, CIM Bulletin 69 (776) (1976) 114–123.

[16] A. C. Silva, E. Maria, S. Silva, J. Diogo, V. Matos, A Modification in Plitts for Hydrocyclones Simulation, Ijrras 13 (December) (2012) 753–758.

[17] K. Nageswararao, D. Wiseman, T. Napier-Munn, Two empirical hydrocyclone models revisited, Minerals Engineering 17 (5) (2004) 671–687. doi:10.1016/j.mineng.2004.01.017.

URL http://linkinghub.elsevier.com/retrieve/pii/S0892687504000731

[18] H. H. Steinour, Rate of sedimentation, Industrial & Engineering Chemistry 36 (9) (1944) 840–847.

[19] K. Nageswararao, A generalized model for hydrocyclone classifiers, in: AusIMM Proceedings, 300, 1995, pp. 21–29.

[20] M. Coelho, R. Medronho, A model for performance prediction of hydrocyclones, Chemical Engineering Journal 84 (1) (2001) 7–14. doi:10.1016/S1385-8947(00)00265-5.
URL http://linkinghub.elsevier.com/retrieve/pii/S1385894700002655

[21] D. F. Kelsall, A further study of the hydraulic cyclone, Chemical Engineering Science 2 (1953) 254–272.
URL http://www.sciencedirect.com/science/article/pii/0009250953800448

[22] D. Bradley, D. J. Pulling, Flow patterns in the hydraulic cyclone and their interpretation in terms of performance, Transactions of the Institution of Chemical Engineers 37 (1959) 34–45.

[23] K. Rietema, Performance and design of hydrocyclones_I, Chem. Eng. Sci. 15 (3-4) (1961) 320–325. doi:10.1016/0009-2509(61)85036-7.
URL http://linkinghub.elsevier.com/retrieve/pii/0009250961850367

[24] K. Rietema, Performance and design of hydrocyclones-II, Chem. Eng. Sci. 15 (3-4) (1961) 298–302.

[25] K. Rietema, Performance and design of hydrocyclones_III, Chemical Engineering Science 15 (3-4) (1961) 310–319. doi:10.1016/0009-2509(61)85035-5.

URL http://linkinghub.elsevier.com/retrieve/pii/0009250961850355

[26] K. Rietema, Performance and design of hydrocyclones-IV, Chemical Engineering Science 15 (3-4) (1961) 320–325. doi:10.1016/0009-2509(61)85036-7.
URL http://linkinghub.elsevier.com/retrieve/pii/0009250961850367

[27] T. Rao, The characteristics of hydrocyclones and their application as control units in comminution circuits, Ph.D. thesis, The University of Queensland (1966).

[28] K. Nageswararao, Modelling and Scale-up of Industrial Hydrocyclones, Ph.D. thesis, The University of Queensland (1978).

[29] A. K. Asomah, Improved Models of Hydrocyclones, Ph.D. thesis, The University of Queensland (1998).

[30] M. Narasimha, Improved Computational and Empirical Models of Hydrocyclones, Ph.D. thesis, The University of Queensland (2009).

[31] A. K. Asomah, T. J. Napier-Munn, An empirical model of hydrocyclones, incorporating angle of cyclone inclination, Minerals Engineering 10 (3) (1997) 339–347. doi:10.1016/S0892-6875(97)00008-3.

[32] M. Narasimha, A. N. Mainza, P. N. Holtham, M. S. Powell, M. S. Brennan, A semi-mechanistic model of hydrocyclones - Developed from industrial data and inputs from CFD, International Journal of Mineral Processing 133 (2014) 1–12. doi:10.1016/j.minpro.2014.08.006.
URL http://dx.doi.org/10.1016/j.minpro.2014.08.006

[33] A. Letki, N. Corner-Walker, Centrifugal separation, Kirk-Othmer Encyclopedia of Chemical Technology 5 (2004) 505–551.

[34] E. Ortega-Rivas, Hydrocyclones, in: Ullmann's Encyclopedia of Industrial Chemistry, Vol. 18, Wiley-VCH Verlag GmbH & Co. KGaA, Weinheim, 2012, pp. 207–233. doi:10.1002/14356007.c13.

[35] S. Kuang, K. Chu, a.B. Yu, a. Vince, Numerical study of liquid-gas-solid flow in classifying hydrocyclones: Effect of feed solids concentration, Minerals Engineeringdoi:10.1016/j.mineng.2012.01.003.
URL http://linkinghub.elsevier.com/retrieve/pii/S0892687512000052

[36] J. H. Masliyah, Hindered settling in a multi-species particle system, Chemical Engineering Science 34 (1979) 1166–1168.

[37] A. Zeidan, S. Rohani, A. Bassi, P. Whiting, Review and comparison of solids settling velocity models, Reviews in Chemical Engineering 19 (5) (2003) 473–530. doi:10.1515/REVCE.2003.19.5.473.

[38] J. F. Richardson, W. N. Zaki, Sedimentation and fluidisation: Part I, Transactions of the Institution of Chemical Engineers 32 (1954) S82–S100. doi:10.1016/S0263-8762(97)80006-8.
URL http://linkinghub.elsevier.com/retrieve/pii/S0263876297800068

[39] H. A. Nasr-el din, J. Masliya, K. Nandakumar, Continuous separation of suspensions containing light and heavy particle species, The Canadian Journal of Chemical Engineering 77 (October) (1999) 1003–1012.

[40] T. E. Baldock, M. R. Tomkins, P. Nielsen, M. G. Hughes, Settling velocity of sediments at high concentrations, Coastal Engineering 51 (1) (2004) 91–100. doi:10.1016/j.coastaleng.2003.12.004.
URL http://linkinghub.elsevier.com/retrieve/pii/S0378383903001340

[41] D. K. Basson, S. Berres, R. Bürger, On models of polydisperse sedimentation with particle-size-specific hindered-settling fac-